Structural Characterization of the Human Eukaryotic Initiation Factor 3 Protein Complex by Mass Spectrometry*

Eugen Damoc‡, Christopher S. Fraser§, Min Zhou¶, Hortense Videler¶, Greg L. Mayeur‖, John W. B. Hershey‖, Jennifer A. Doudna§, Carol V. Robinson¶**, and Julie A. Leary‡ ‡‡

Protein synthesis in mammalian cells requires initiation factor eIF3, an ~800-kDa protein complex that plays a central role in binding of initiator methionyl-tRNA and mRNA to the 40 S ribosomal subunit to form the 48 S initiation complex. The eIF3 complex also prevents premature association of the 40 and 60 S ribosomal subunits and interacts with other initiation factors involved in start codon selection. The molecular mechanisms by which eIF3 exerts these functions are poorly understood. Since its initial characterization in the 1970s, the exact size, composition, and post-translational modifications of mammalian eIF3 have not been rigorously determined. Two powerful mass spectrometric approaches were used in the present study to determine post-translational modifications that may regulate the activity of eIF3 during the translation initiation process and to characterize the molecular structure of the human eIF3 protein complex purified from HeLa cells. In the first approach, the bottom-up analysis of eIF3 allowed for the identification of a total of 13 protein components (eIF3a–m) with a sequence coverage of ~79%. Furthermore 29 phosphorylation sites and several other post-translational modifications were unambiguously identified within the eIF3 complex. The second mass spectrometric approach, involving analysis of intact eIF3, allowed the detection of a complex with each of the 13 subunits present in stoichiometric amounts. Using tandem mass spectrometry four eIF3 subunits (h, i, k, and m) were found to be most easily dissociated and therefore likely to be on the periphery of the complex. It is noteworthy that none of these four subunits were found to be phosphorylated. These data raise interesting questions about the function of phosphorylation as it relates to the core subunits of the complex. ***Molecular & Cellular Proteomics 6:1135–1146, 2007.***

From the ‡Genome Center, Departments of Chemistry and Molecular Cell Biology, University of California, Davis, California 95616, the §Department of Molecular and Cell Biology, University of California, Berkeley, California 94720, the ¶Department of Chemistry, University of Cambridge, Cambridge CB2 1EW, United Kingdom, and the ‖Department of Biochemistry and Molecular Medicine, School of Medicine, University of California, Davis, California 95616

Received, October 16, 2006, and in revised form, February 16, 2007
Published, MCP Papers in Press, February 23, 2007, DOI 10.1074/mcp.M600399-MCP200

The initiation phase of eukaryotic protein synthesis involves formation of an 80 S ribosomal complex containing the initiator methionyl-tRNA$_i$ bound to the initiation codon in the mRNA. This is a multistep process promoted by proteins called eukaryotic initiation factors (eIFs).[1] Currently at least 12 eIFs, composed of at least 29 distinct subunits, have been identified (1). Mammalian eIF3, the largest initiation factor, is a multisubunit complex with an apparent molecular mass of ~800 kDa. This protein complex plays an essential role in translation by binding directly to the 40 S ribosomal subunit and promoting formation of the 43 S preinitiation complex consisting of the Met-tRNA$_i$·eIF2·GTP ternary complex, eIF1, eIF1A, and the 40 S ribosomal subunit (2, 3). The ability of eIF3 to bind to 40 S subunits in the absence of other initiation factors is enhanced by the presence of its loosely associated eIF3j subunit (4). The eIF3 complex also promotes binding of 5′-m^{7}G-capped mRNA through its interaction with eIF4G, the largest member of the eIF4F cap-binding complex (5, 6). The 43 S preinitiation complex then scans the mRNA (together forming the 48 S complex) in a 5′ to 3′ direction until the initiation codon AUG is selected. Upon recognition of the initiation codon, eIF5 stimulates hydrolysis of the GTP bound to eIF2, and the eIFs are ejected from the ribosome. The 60 S ribosomal subunit then joins the 40 S initiation complex aided by eIF5B (7).

Mammalian eIF3 consists of 13 non-identical subunits that range in size from 170 to 25 kDa and are named eIF3a through eIF3m (8, 9). Characterization of eIF3 in mammalian cells has been hampered by its large size and complexity, and only recently have the cDNAs been cloned and sequenced for all of the subunits (9, 10). The functions of the individual subunits are not yet well established. In the yeast *Saccharomyces cerevisiae*, eIF3 appears to consist of a core complex of only five stoichiometric subunits (eIF3a, -b, -c, -g, and -i), plus a non-stoichiometric subunit, eIF3j. In mammalian cells, the corresponding homologs also may constitute a "core" complex to which the other mammalian subunits bind and regulate eIF3 activity. Interestingly two forms of eIF3 occur in the fission yeast *Schizosaccharomyces pombe*. Both forms share the five core subunits plus eIF3f, but one contains exclusively the eIF3h and eIF3m

[1] The abbreviations used are: eIF, eukaryotic initiation factor; nano-LC, nanospray LC; IAA, iodoacetamide; DMEM, Dulbecco's modified Eagle's medium; PTM, post-translational modification; LTQ, linear quadrupole ion trap.

subunits, whereas the other contains the eIF3d and eIF3e subunits (11). It is not yet clear whether mammalian eIF3 exists as multiple forms containing different sets of subunits.

Yeast eIF3 interacts with eIF1, eIF2β, and eIF5 to form a multifactor complex (12, 13). Mammalian eIF3 also binds eIF1 and eIF5 (14–16) and, in addition, binds eIF4B (17) and eIF4G (18). Most of these interactions have been mapped to individual eIF3 subunits. In *S. cerevisiae* for example, eIF1 binds eIF3a and eIF3c (19, 20), eIF5 binds eIF3c (19), and eIF2β binds eIF3a (20). In mammals, eIF1 binds eIF3c (21), and eIF5 interacts with eIF3c (22). Finally eIF4B binds eIF3a in mammals (17) and eIF3g in *S. cerevisiae* (23) and plants (24), whereas eIF4G binds to eIF3e in mammals (25).

Together with its RNA binding activity and its ability to bind stably to the 40 S ribosome, mammalian eIF3 clearly plays a central role in the initiation pathway possibly as an organizer of other initiation factors on the surface of the 40 S ribosomal subunit. Some insight into the function of human eIF3 comes from a low resolution structure determined by cryoelectron microscopy that depicts eIF3 as an anthropomorphic structure with five domains named according to body parts (26). Modeling the structure on the 40 S ribosomal subunit places eIF3 on the solvent side of the ribosome similar to the position observed by negative stain electron microscopy (27) with two of the appendages reaching around to the interface side where Met-tRNA$_i$ binding and initiation codon decoding occurs. However, the composition of each of the five appendages is not yet known, and the molecular mechanisms by which eIF3 exerts its functions are poorly understood.

The hypothesis that eIF3 activity is regulated in mammalian cells is based on the fact, reported here, that a number of its subunits are phosphoproteins and that phosphorylation of eIF3 is stimulated by treatment of cells with serum. Most other initiation factors are phosphoproteins (28, 29), and phosphorylation has been shown to function as a general mechanism for the regulation of initiation (29). These facts have precipitated a mass spectrometry-based study to characterize the molecular structure of the eIF3 protein complex. The study includes the identification of post-translational modifications that may modulate its activity during the translation initiation process. For the first time, data collected reveals the mass of the intact 13 subunit complex. Although other small molecules or ancillary proteins may be associated with the eIF3 complex, only those 13 proteins comprising the complex are investigated in detail herein.

The relatively recent development of efficient "soft ionization" methods has provided the basis for the molecular characterization of biopolymers by mass spectrometry. ESI-MS has become a powerful molecular tool for protein primary structure determination (30, 31), the study of conformational states and folding pathways (32), the characterization of noncovalent supramolecular complexes (33, 34), and the analysis of complex mixtures by combination with microseparation methods (HPLC and capillary electrophoresis) (35, 36). Recently ESI-MS has been used to analyze macromolecular assemblies of increasing size and complexity (37, 38).

In the present study two different mass spectrometric approaches were used to provide information on the molecular structure of the human eIF3 protein complex purified from HeLa cells and to determine post-translational modifications (*e.g.* phosphorylation) that may regulate its activity during the translation initiation process. Nanospray (nano-) LC-MS/MS analysis of an eIF3 tryptic digest using a hybrid linear ion trap-FTICR mass spectrometer was used for the identification of eIF3 protein subunits and their corresponding post-translational modifications. Due to the dynamic nature and low stoichiometry of protein phosphorylation, enrichment of phosphorylated peptides from eIF3 proteolytic mixture using Ga(III) IMAC and TiO_2 (39) was used prior to their characterization to obtain accurate data on the number and sites of phosphorylation. In the second approach, a high mass Q-TOF type instrument (40–42) was used to analyze the intact eIF3 complex to obtain stoichiometry as well as identification of the peripheral subunits within the eIF3 complex.

EXPERIMENTAL PROCEDURES

Materials—Iodoacetamide (IAA) and DTT were obtained from Sigma. Trypsin was purchased from Promega (Madison, WI). Minispin columns containing SwellGel™ gallium-chelated discs were obtained from Pierce. Microtips filled with TiO_2 were purchased from Glygen (Columbia, MD). All other chemicals were analytical grade purchased from Fisher and used without further purification.

In Vivo Phosphorylation of eIF3—HeLa cells were grown in Dulbecco's modified Eagle's medium (DMEM) supplemented with 10% FCS. Cells were washed twice with phosphate-free DMEM lacking serum and placed in phosphate-free DMEM supplemented with 0.5% heat-inactivated horse serum for 24 h prior to labeling. Cells were loaded with [^{32}P]orthophosphate (0.5mCi/ml) for 4 h prior to stimulation by the addition of 10% FCS. At various times following the addition of FCS, cells were placed on ice and washed twice in ice-cold PBS and lysed in Nonidet P-40 lysis buffer containing phosphatase and protease inhibitors (1% Nonidet P-40, 50 mM Tris-HCl, pH 7.4, 50 mM KCL, 50 mM β-glycerol phosphate, 50 mM NaF, 2 mM EGTA, 0.2 mM benzamidine, 1 mM Na_3VO_4, 7.5 mM 2-mercaptoethanol, Roche Applied Science Complete protease inhibitor mixture). Protein levels were quantified by using the BCA protein assay reagents (Pierce). Equal amounts of lysate protein were immunoprecipitated with goat anti-eIF3 antibodies followed by protein G-agarose. The immunoprecipitates were fractionated by SDS-PAGE followed by autoradiography to detect phosphoproteins.

Purification of eIF3—Postnuclear HeLa cell lysates were a kind gift from Eva Nogales (Howard Hughes Medical Institute, University of California, Berkeley, CA). For each preparation, 400 ml of HeLa extract (~150 g of cells) was thawed quickly in a 37 °C water bath and supplemented with the following (final concentrations): 10% glycerol, 1 mM EDTA, 1 mM EGTA, 50 mM NaF, 50 mM β-glycerol phosphate, 10 mM benzamidine, 1 mM PMSF, 1× protease inhibitor mixture (Roche Applied Science). The resulting lysate was clarified by centrifugation at 20,000 × *g* for 20 min at 4 °C followed by addition of KCl to a final concentration of 450 mM. The lysate was then centrifuged in a Ti45 rotor at 45,000 rpm for 4 h at 4 °C. The middle two-thirds of the supernatant was carefully removed and stirred in a beaker at 4 °C with the slow addition of saturated ammonium sulfate (pH 7.5) to a final concentration of 40% saturation. After stirring at 4 °C for 1 h, the precipitate was recovered by centrifugation at 20,000 × *g* for 10 min at 4 °C. The precipitate was resuspended in 50 ml of buffer A (20 mM Hepes, pH 7.5, 10% glycerol, 1 mM EDTA, 1 mM EGTA, 50 mM NaF, 50 mM β-glycerol phosphate, 10 mM benzamidine, 1 mM DTT) containing 50 mM KCl and dialyzed in 2 liters of the same buffer for 2.5 h at 4 °C. Following dialysis the lysate was passed through a 0.2-μm

filter and loaded onto a Mono Q (10/10) column (GE Healthcare) equilibrated in buffer A containing 100 mM KCl. The column was eluted with a 120-ml gradient from 100 to 600 mM KCl in buffer A at 2 ml/min, and 3-ml fractions were collected. The fractions containing eIF3 were identified by SDS-PAGE, pooled, dialyzed into buffer A containing 100 mM KCl for 2.5 h at 4 °C, and loaded onto a Mono S (10/10) column (GE Healthcare) equilibrated in the same buffer. The column was eluted with a 120-ml 100–400 mM KCl gradient in buffer A at 2 ml/min, and 3-ml fractions were collected. The fractions containing eIF3 were pooled, concentrated using an Amicon Ultra filtration device to 1.5 ml, and loaded onto a Superose 6 (16/60) column (GE Healthcare) equilibrated in buffer A containing 100 mM KCl (except that 10 mM NaF and 10 mM β-glycerol phosphate were used). The column was run at 0.3 ml/min, and 1-ml fractions were collected. The fractions containing eIF3 were pooled and concentrated using an Amicon Ultra filtration device to a final concentration of between 1 and 2 mg/ml. A one-dimensional gel of the eIF3 preparation is provided in the supplemental material.

Acetone Precipitation—Acetone precipitation was used to remove LC-MS-interfering species from the eIF3 sample. The purified eIF3 protein complex was precipitated at −20 °C for 8 h by adding 6 volumes of ice-cold acetone to the eIF3 sample solution. After a 20-min centrifugation at 13,200 rpm the residual acetone was removed, and the eIF3 pellet was allowed to air dry.

In-solution Tryptic Digestion of eIF3 Protein Complex—Acetone-precipitated eIF3 (100 μg of protein) was first reduced at 56 °C for 45 min in a 270-μl solution of 50 mM ammonium bicarbonate and 5.5 mM DTT and then *S*-alkylated in the dark at room temperature for 1 h by adding a 30-μl solution of 100 mM IAA. Trypsin was added to the protein in a final enzyme:substrate ratio of 1: 50, and the digestion was carried out at 37 °C for 2 h. The reaction was quenched by freezing the sample with liquid nitrogen. The eIF3 tryptic digest was then lyophilized.

Enrichment of Phosphopeptides from the eIF3 Tryptic Digest by Ga(III) IMAC—Mini-spin columns containing SwellGel gallium-chelated discs (Pierce) were used for the enrichment of eIF3 phosphopeptides as recommended by the manufacturer. Briefly 50 μg of the lyophilized eIF3 tryptic digest was dissolved in 20 μl of 10% acetic acid. The sample was then applied to the column and washed two times with 50 μl of 0.1% acetic acid followed by two times with 50 μl of 0.1% acetic acid in 10% ACN and ending with one time with 75 μl of MilliQ water. The sample was then eluted in three steps using 1) 20 μl of 100 mM ammonium bicarbonate, 2) 20 μl of 100 mM ammonium bicarbonate in 10% ACN, and 3) 20 μl of 100 mM ammonium bicarbonate in 20% ACN. All three fractions were mixed, dried down, and reconstituted in a solution of 2% ACN in 0.1% TFA just prior to nano-LC-MS/MS analysis.

Enrichment of Phosphopeptides from eIF3 Tryptic Digest Using TiO_2—Microtips filled with TiO_2 were purchased from Glygen and used according to the manufacturer's instructions. Briefly 50 μg of the lyophilized eIF3 tryptic digest was reconstituted in 25 μl of a solution of 0.1% TFA containing 10% ACN and loaded onto microtips that had been equilibrated previously with the same solution. Unbound peptides were removed by washing the packed bed with 50 μl of 0.1% TFA containing 10% ACN and then with 2 × 50 μl of MilliQ water. Bound peptides were eluted with 3 × 25 μl of 200 mM NH_4OH. Eluted peptide samples were dried down and reconstituted in a solution of 2% ACN in 0.1% TFA just prior to nano-LC-MS/MS analysis.

Nano-LC-MS/MS and MS^3 Analysis of eIF3 Tryptic Digest—Nano-LC tandem mass spectrometric analysis was performed on an LTQ-FT hybrid linear ion trap/7-tesla Fourier transform ion cyclotron resonance mass spectrometer (Thermo Electron, San Jose, CA) equipped with a nanospray ion source (Thermo Electron), a Surveyor MS pump (Thermo Electron), and a microautosampler (Thermo Electron). The lyophilized eIF3 tryptic peptide mixture was dissolved in 2% ACN in 0.1% TFA and separated on a 50-μm-inner diameter PicoFrit column packed in house with Magic C18AQ material (Michrom BioResources, Inc., Auburn, CA). The column was packed to a length of 12 cm with a 100% MeOH slurry of C_{18} reversed-phase material (100-Å pore size, 3-μm particle size) using a high pressure cell pressurized with helium. The column was equilibrated before sample injection for 10 min at 2% solvent B (0.1% (v/v) formic acid in ACN) and 98% solvent A (0.1% (v/v) formic acid in water) at a flow rate of 140 nl/min. Separation was achieved by using a linear gradient from 2 to 50% solvent B in 110 min at a flow rate of 320 nl/min. The LTQ-FT mass spectrometer was operated in the data-dependent acquisition mode using the TOP10 and the neutral loss/MS^3 method.

By using the TOP10 method, survey full-scan MS spectra (from *m/z* 300 to 1600) were acquired in the FTICR mass spectrometer with resolution $r = 100{,}000$ at *m/z* 400 (after accumulation to a target value of 10^6 ions in the linear ion trap) and were followed by 10 MS^2 experiments performed with the LTQ (at a target value of 10^4 ions) on the 10 most abundant ions detected in the full-scan MS. The MS/MS isolation width was 2.0 Da, and the normalized collision energy was 35%. Former target ions selected for MS/MS were dynamically excluded for 45 s.

For the neutral loss-dependent MS^3 acquisition, survey full-scan MS spectra (from *m/z* 300 to 1400) were acquired by FTICR with resolution $r = 100{,}000$ at *m/z* 400 (after accumulation to a target value of 10^6 ions in the linear ion trap) and were followed by CID fragmentation of the five most intense ions in the linear ion trap (at a target value of 10^4 ions). The data-dependent neutral loss algorithm in the Xcalibur software was enabled for each MS^2 spectra. Data-dependent settings were chosen to trigger an MS^3 event in the linear ion trap (at a target value of 10^4 ions) when a neutral loss of 98, 49, or 32.7 Da (H_3PO_4 for the 1+, 2+, and 3+ charged ions, respectively) was detected among the five most intense fragment ions.

Database Search—The raw data files acquired for each LC-MS run were converted to MASCOT generic files using extract_MSN software. The resulting MASCOT generic files were searched against UniProtKB/Swiss-Prot 49.4 (215,741 sequence entries) and National Center for Biotechnology Information non-redundant (NCBInr) April 14, 2006 (3,570,920 sequence entries) databases using the MASCOT search engine (version 2.1.03, Matrix Science Ltd.). Searches were done with tryptic specificity allowing four missed cleavages and a tolerance on the mass measurement of 20 ppm in MS mode and 0.5 Da for MS/MS ions. Possible structure modifications allowed were carbamidomethylation of Cys; oxidation of Met; deamidation of Asn and Gln; phosphorylation of Ser, Thr, and Tyr; and protein N-terminal acetylation. The matches for MS/MS data were generally accepted only when the scoring value exceeded the identity or extensive homology threshold. When scores were lower than this threshold, manual inspection of the raw data was used for confirmation prior to acceptance. Phosphorylation sites contained in MASCOT search results were all validated by manual confirmation from raw MS^2 and MS^3 data. Each confirmed phosphorylated eIF3 subunit was searched with Scansite (53) for potential kinase motifs with high, medium, and low stringency. For all PTMs reported here, the supporting CID spectra are presented in the supplemental material and Figs. 2 and 3 with the exception of the N-terminal protein acetylation of the eIF3f subunit. This PTM was identified based on the accurate *m/z* measured by FTMS, and the FTMS spectrum is shown in the supplemental material.

Mass Spectrometric Analysis of the Intact eIF3 Protein Complex—Mass spectra collected for the intact protein complexes were recorded on a QSTAR XL mass spectrometer (MDS Sciex) modified for high mass detection (40). The eIF3 complex (1 μg/μl) was buffer-exchanged into 100 mM ammonium acetate (pH 7.5) and 1 mM dithiothreitol using Micro Biospin 6 columns (Bio-Rad), and 2-μl aliquots

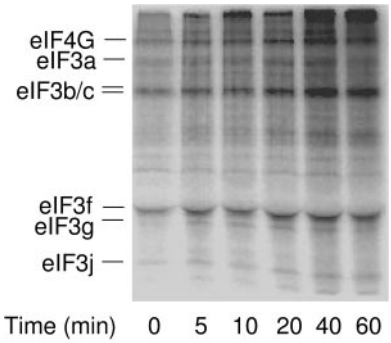

FIG. 1. **Autoradiogram showing that phosphorylation of eIF3a, eIF3b, eIF3c, eIF3f, eIF3g, and eIF3j subunits is stimulated by treatment of HeLa cells with serum.** Serum-deprived HeLa cells were treated with [^{32}P]orthophosphate and then stimulated with fetal bovine serum as described under "Experimental Procedures." At various times, cell lysates were prepared, subjected to immunoprecipitation with anti-eIF3 antibodies, and analyzed by SDS-PAGE. The figure shows an autoradiogram of the gel. Bands corresponding to eIF3 subunits and eIF4G are labeled on the *left*.

were introduced via nanoflow capillaries prepared in house. The conditions within the mass spectrometer were adjusted to preserve non-covalent interactions. The mass spectrometer was operated at a capillary voltage of 1200 V and a declustering potential of 40 V. An MS/MS spectrum of the intact eIF3 complex was obtained by tandem mass spectrometry of a broad isolation at 12,200 *m/z* with collision energy of 150 V.

RESULTS AND DISCUSSION

In Vivo Phosphorylation of Human eIF3—Although phosphorylation of initiation factors has long been recognized as a means to regulate translation, little attention has been given to characterizing eIF3 in this regard. An early report identified eIF3-p115 as a phosphoprotein (43), but it was not recognized that the p115 band contained two eIF3 subunits, eIF3b and eIF3c. To more completely characterize the phosphorylation state of eIF3, HeLa cells were treated with [^{32}P]orthophosphate under conditions of serum deprivation and then stimulated with fetal bovine serum. Cell lysates were subjected to immunoprecipitation with anti-eIF3 antibodies and analysis by SDS-PAGE. The autoradiogram shown in Fig. 1 shows strong bands corresponding to eIF3a, eIF3b, eIF3c, eIF3f, and eIF3j with a weak band for eIF3g. These bands are about 3-fold more intense following serum stimulation, indicating that eIF3 phosphorylation correlates with activation of protein synthesis. We conclude that eIF3 is phosphorylated on multiple subunits and may be regulated by this post-translational modification reaction. It was therefore important to identify the sites of phosphorylation to study how the activity of the factor might be controlled. This was performed using the mass spectrometry assays described below.

Nano-LC-MS/MS and MS^3 Analysis of the eIF3 Tryptic Digest—The human eIF3 protein complex purified from HeLa cells was precipitated with acetone and then reduced with DTT, alkylated with IAA, and digested with trypsin. The resulting eIF3 tryptic peptide mixture was injected into a nano-LC C_{18} column coupled to a hybrid linear ion trap-FTICR mass spectrometer, and the MS/MS and MS^3 analysis was carried out using data-dependent acquisition mode as described under "Experimental Procedures." All MS/MS spectra were searched against UniProtKB/Swiss-Prot and NCBInr databases using the MASCOT search engine, and 13 protein components of human eIF3 complex were unambiguously identified. The 13th subunit (eIF3m) is identified as GA17, a 42.5-kDa protein that contains a PCI domain (44), a domain found in five other eIF3 subunits (a, c, e, k, and l) and in subunits of the proteasome lid and COP9 signalosome. This protein was reported previously to be part of the eIF3 from HeLa cells and rabbit reticulocytes based on the identification of only three tryptic peptides covering 9% of the protein sequence (9). In the present study, a sequence coverage of 74% was obtained for the eIF3m subunit (see the supplemental material), and its N terminus was found to have lost the methionine residue with subsequent formation of a new N terminus as an *N*-acetylated serine. Approximately 79% sequence coverage of the entire human eIF3 complex was obtained using the high mass accuracy and fast MS/MS capabilities of the LTQ-FT mass spectrometer in combination with on-line nanoflow LC separation. The sequence coverage of each of the 13 eIF3 subunits is shown in the supplemental material. A total of 29 phosphorylation sites were identified within the eIF3a, eIF3b, eIF3c, eIF3f, eIF3g, eIF3h, and eIF3j subunits of which nine phosphorylation sites were identified only when selective enrichment of phosphopeptides by TiO_2 and Ga(III) IMAC was carried out (see Tables I and II). Of the 29 eIF3 phosphorylation sites identified in this study, eight were reported previously and could be found in PhosphoSite (Cell Signaling Technology) and UniProt (www.expasy.uniprot.rot.org) databases. The phosphorylation sites Ser-83, Ser-85, and Ser-125 from eIF3b; Ser-166 and Thr-524 from eIF3c; and Ser-42 from the eIF3g were identified previously in the HeLa cell nuclear fraction by Gygi and co-workers (45). Two other eIF3c phosphorylation sites were reported after global phosphoproteome analysis of human HepG2 hepatocytes (Ser-39) (46) and HT-29 human colon adenocarcinoma cells (Ser-909) (47). Several other post-translational modifications of human eIF3 protein subunits such as loss of N-terminal methionine and/or N-terminal protein acetylation were also identified in this study, and all identifications are presented in Tables I and II.

For the correct identification of eIF3 phosphopeptides and corresponding phosphorylation sites, the neutral loss-dependent MS^3 mode of operation of the LTQ was used in addition to the TOP10 method. During fragmentation of the Ser-/Thr-phosphorylated peptides under CID conditions, the main fragmentation pathway is gas-phase elimination of phosphoric acid with the subsequent conversion of phosphoserine and phosphothreonine to dehydroalanine and 2-aminodehydrobutyric acid, respectively. MS^3 experiments, as developed by Gygi and co-workers (45), were triggered whenever loss of phosphoric acid

TABLE I
Identification of eIF3 protein subunits and their corresponding PTMs using nano-LC-LTQ-FTMS

Protein name	UniProt accession number	Molecular mass[a]	Sequence coverage	Post-translational modifications[b]
		Da	%	
eIF3a	Q14152	166,758.3	86	Loss of Met-1, phosphorylation (Ser-881, Ser-1198, Ser-1336*, Ser-1364*)
eIF3b	P55884	93,093.7	77	Acetylation (Met-1), phosphorylation (Ser-83, Ser-85, Ser-119, Ser-125*, Ser-152, Ser-154, Ser-164)
eIF3c	Q99613	106,143.8	65	Phosphorylation (Ser-9, Ser-11, Ser-13, Ser-15, Ser-16, Ser-18, Ser-39, Ser-166**, Thr-524*, Ser-909**)
eIF3d	O15371	63,972.9	74	Not found
eIF3e	P60228	52,131.8	84	Loss of Met-1, acetylation (Ala-2)
eIF3f	O00303	37,554.8	79	Loss of Met-1, acetylation (Ala-2), phosphorylation (Ser-258*)
eIF3g	O75821	35,639.8	83	Loss of Met-1, phosphorylation (Thr-41, Ser-42)
eIF3h	O15372	40,010.4	89	Phosphorylation (Ser-183*)
eIF3i	Q13347	36,501.9	93	Not found
eIF3j	O75822	29,293.2	81	Loss of Met-1, acetylation (Ala-2), phosphorylation (Ser-11, Ser-13, Ser-20, Thr-109**)
eIF3k	Q9UBQ5	24,970.6	75	Loss of Met-1, acetylation (Ala-2)
eIF3l	Q9Y262	66,637.9	70	Loss of Met-1, acetylation (Ser-2)
eIF3m	Q7L2H7	42,413.8	74	Loss of Met-1, acetylation (Ser-2)

[a] Calculated from the theoretical average mass of the corresponding eIF3 protein subunit plus any post-translational modifications identified.
[b] *, found only after TiO_2 phosphopeptide enrichment **, found only after Ga(III) IMAC or TiO_2 phosphopeptide enrichment.

was detected. The result, in many cases, was a richer fragmentation spectrum from which the phosphopeptide sequence could be determined, including the modified residue (Ser or Thr). Jensen and co-workers (48) have applied the same strategy on a hybrid linear ion trap-FTICR mass spectrometer that has the advantage of faster scan speeds, accurate mass measurements of precursor ions, and better storage of precursor ions. The result is that the MS^3 spectra are both richer in information and much faster to acquire. In particular, the large dynamic range of the LTQ allows observation of low level, but significant, ions in the MS^3 spectra.

An example highlighting the neutral loss/MS^3 method for the identification of the phosphorylated Ser-39 from the eIF3c is shown in Fig. 2. At an elution time of 31.8 min (Fig. 2*A*), a precursor ion was observed in the FTICR survey scan (Fig. 2*B*) with a 2+ charge state and a monoisotopic mass at *m/z* of 876.9062 (Δm = 0.7 ppm). This ion was automatically isolated in the linear ion trap and fragmented by CID to produce the MS^2 spectrum (Fig. 2*C*) from which the fifth most intense ion corresponding to the neutral loss precursor ion (*m/z* = 827.91) was again automatically selected and fragmented to yield an MS^3 spectrum (Fig. 2*D*). The tryptic phosphopeptide (amino acids 34–47) was unambiguously identified by the MASCOT search with a top score of 79 (where a score greater than 35 indicates identity), and Ser-39 was identified as being phosphorylated based on the b and y fragment ions present in the MS/MS spectrum. The same amino acid residue was converted, after neutral loss of H_3PO_4, to dehydroalanine as demonstrated by a predominant series of b and y fragment ions present in the MS^3 spectrum.

The hexaphosphorylated tryptic peptide (amino acids 4–33) from the N-terminal region of the eIF3c subunit was also identified by the MASCOT search with a top score of 51 (a score greater than 27 indicates identity), and all six phosphorylation sites (Ser-9, Ser-11, Ser-13, Ser-15, Ser-16, and Ser-18) were unambiguously determined as shown by MS/MS data (Fig. 3). The FTMS survey scan revealed the $[M + 3H]^{3+}$ ion (see Fig. 3, *upper right side*) with the monoisotopic mass *m/z* of 1197.0900 (Δm = 2.0 ppm). A total of seven serine residues (Ser-9, Ser-11, Ser-13, Ser-15, Ser-16, Ser-18, and Ser-39) from the N-terminal domain of the eIF3c were found to be phosphorylated, and the potential kinases responsible for their phosphorylation were predicted by Scansite to be the acidophilic serine kinases, casein kinase 1 or 2. This multiphosphorylation may be involved in the binding of eIF3c to eIF1 through one of the eIF1 clusters of positively charged residues and/or to the eIF5 through its positively charged amino acids Lys-357, Lys-360, Lys-361, Lys-365, Lys-369, and Arg-382 (22). This sequence of experiments was utilized to identify each of the proteins and a large number of phosphorylation sites within the subunits (Table II). It remains possible that additional phosphorylation sites will be found either in protein regions not covered by the MS analyses reported here or in covered regions that either have lost the phosphates during eIF3 purification or were not phosphorylated under the physiological conditions used to grow the HeLa cells and prepare the eIF3. For example, eIF3f is phosphorylated on Ser-46 by $CDK11^{p46}$ when activated during apoptosis (49). Future studies will focus on quantitative methods to determine stoichiometry of the identified phosphorylations as this was not determined for this particular sample preparation.

Mapping of eIF3 phosphorylation sites represents one step further in the elucidation of the possible role of phosphorylation in the regulation of eIF3 activity in translation. Such map-

TABLE II

Phosphopeptides and corresponding phosphorylation sites identified in eIF3 tryptic digest using nano-LC-LTQ-FTMS

*, N-terminal protein acetylation; DDA, data-dependent acquisition; NL, neutral loss. Shading denotes phosphorylation sites

sequence	eIF3 subunit	start-end	no. of PO_4	$[M+H]^+$ (Da)	charge states	site(s) identified	DDA method		enrichment method		without enrich-ment
							TOP10	NL/ MS3	TiO_2	Ga(III) IMAC	
RLGDSSLSR	a	877-885	1	1070.4996	2+	Ser-881	yes	yes	yes	yes	yes
ESRPSEEREWDR	a	1194-1205	1	1655.6816	3+	Ser-1198	yes	yes	yes	no	no
ESRPSEEREWDREK	a	1194-1207	1	1912.8191	2+, 3+	Ser-1198	no	yes	yes	no	yes
RVPPPALSR	a	1329-1337	1	1072.5669	2+	Ser-1336	yes	yes	yes	no	no
RVPPPALSRDR	a	1329-1339	1	1343.6950	2+, 3+	Ser-1336	yes	yes	yes	no	no
AEKDRESLRR	a	1358-1367	1	1339.6484	2+, 3+	Ser-1364	yes	yes	yes	no	no
TEPAAEAEAASGPSESPSPP AAEELPGSHAEPPVPAQGE APGEQAR	b	68-113	1	4538.0273	4+, 5+, 6+	Ser-83	yes	no	yes	yes	yes
TEPAAEAEAASGPSESPSPP AAEELPGSHAEPPVPAQGE APGEQAR	b	68-113	2	4617.9937	4+, 5+, 6+	Ser-83, Ser-85	yes	no	yes	yes	yes
SDSRAQAVSEDAGGNEGR	b	117-134	1	1885.7678	2+, 3+	Ser-119	yes	yes	yes	yes	yes
AQAVSEDAGGNEGR	b	121-134	1	1440.5757	2+	Ser-125	yes	no	yes	no	no
ALENGDADEPSFSDPEDFV DDVSEEELLGDVLK	b	142-174	1	3675.5639	3+	Ser-152	yes	yes	yes	yes	yes
ALENGDADEPSFSDPEDFV DDVSEEELLGDVLK	b	142-174	2	3755.5302	3+	Ser-152, Ser-154	yes	yes	yes	yes	yes
ALENGDADEPSFSDPEDFV DDVSEEELLGDVLK	b	142-174	3	3835.4966	3+	Ser-152, Ser-154, Ser-164	yes	yes	yes	no	yes
FFTTGSDSESESSLSGEELV TKPVGGNYGK	c	4-33	6	3589.2470	3+	Ser-9, Ser-11, Ser-13, Ser-15, Ser-16, Ser-18	yes	yes	no	no	yes
QPLLLSEDEEDTK	c	34-46	1	1596.7046	2+	Ser-39	yes	yes	yes	yes	no
QPLLLSEDEEDTKR	c	34-47	1	1752.8058	2+, 3+	Ser-39	yes	yes	yes	yes	yes

TABLE II—*continued*

QNPEQSADEDAEK	c	161-173	1	1580.5805	2+	Ser-166	yes	no	yes	yes	no
QLTPPEGSSK	c	522-531	1	1123.5037	2+	Thr-524	yes	no	yes	no	no
QQQSQTAY	c	906-913	1	1033.3992	2+	Ser-909	yes	no	yes	yes	no
TCFSPNR	f	255-261	1	961.3603	2+	Ser-258	yes	yes	yes	no	no
GIPLATGDTSPEPELLPGAPLPPPK	g	33-57	1	2544.3003	2+, 3+	Ser-42	yes	yes	yes	yes	yes
GIPLATGDTSPEPELLPGAPLPPPKEVINGNIK	g	33-65	1	3411.7817	3+	Ser-42	yes	no	yes	yes	yes
GIPLATGDTSPEPELLPGAPLPPPKEVINGNIK	g	33-65	2	3491.7480	3+	Thr-41, Ser-42	yes	yes	yes	no	yes
DFSPEALKK	h	181-189	1	1114.5186	2+	Ser-183	no	yes	yes	no	no
EKDFSPEALKK	h	179-189	1	1371.6562	2+	Ser-183	yes	yes	yes	no	no
*AAAAAAAGDSDSWDADAFSVEDPVR	j	2-26	1	2587.0626	2+, 3+	Ser-11	yes	no	yes	yes	yes
*AAAAAAAGDSDSWDADAFSVEDPVR	j	2-26	2	2667.0290	3+	Ser-11, Ser-13	yes	no	no	yes	yes
*AAAAAAAGDSDSWDADAFSVEDPVR	j	2-26	3	2746.9953	3+	Ser-11, Ser-13, Ser-20	yes	no	no	yes	yes
*AAAAAAAGDSDSWDADAFSVEDPVRK	j	2-27	1	2715.1576	2+, 3+	Ser-11	yes	yes	yes	yes	yes
*AAAAAAAGDSDSWDADAFSVEDPVRK	j	2-27	2	2795.1239	3+	Ser-11, Ser-13	yes	yes	yes	yes	no
LEEPEEPKVLTPEEQLADK	j	99-117	1	2274.0795	3+	Thr-109	yes	no	yes	yes	no
VLTPEEQLADKLR	j	107-119	1	1591.8097	2+	Thr-109	yes	yes	yes	yes	no
VLTPEEQLADK	j	107-117	1	1322.6245	2+	Thr-109	no	yes	yes	no	no
LEEPEEPKVLTPEEQLADKLR	j	99-119	1	2543.2646	3+	Thr-109	no	yes	yes	no	no
RLEEPEEPKVLTPEEQLADK	j	98-117	1	2430.1806	3+	Thr-109	yes	yes	yes	no	no
RLEEPEEPKVLTPEEQLADKLR	j	98-119	1	2699.3658	3+	Thr-109	no	yes	yes	no	no

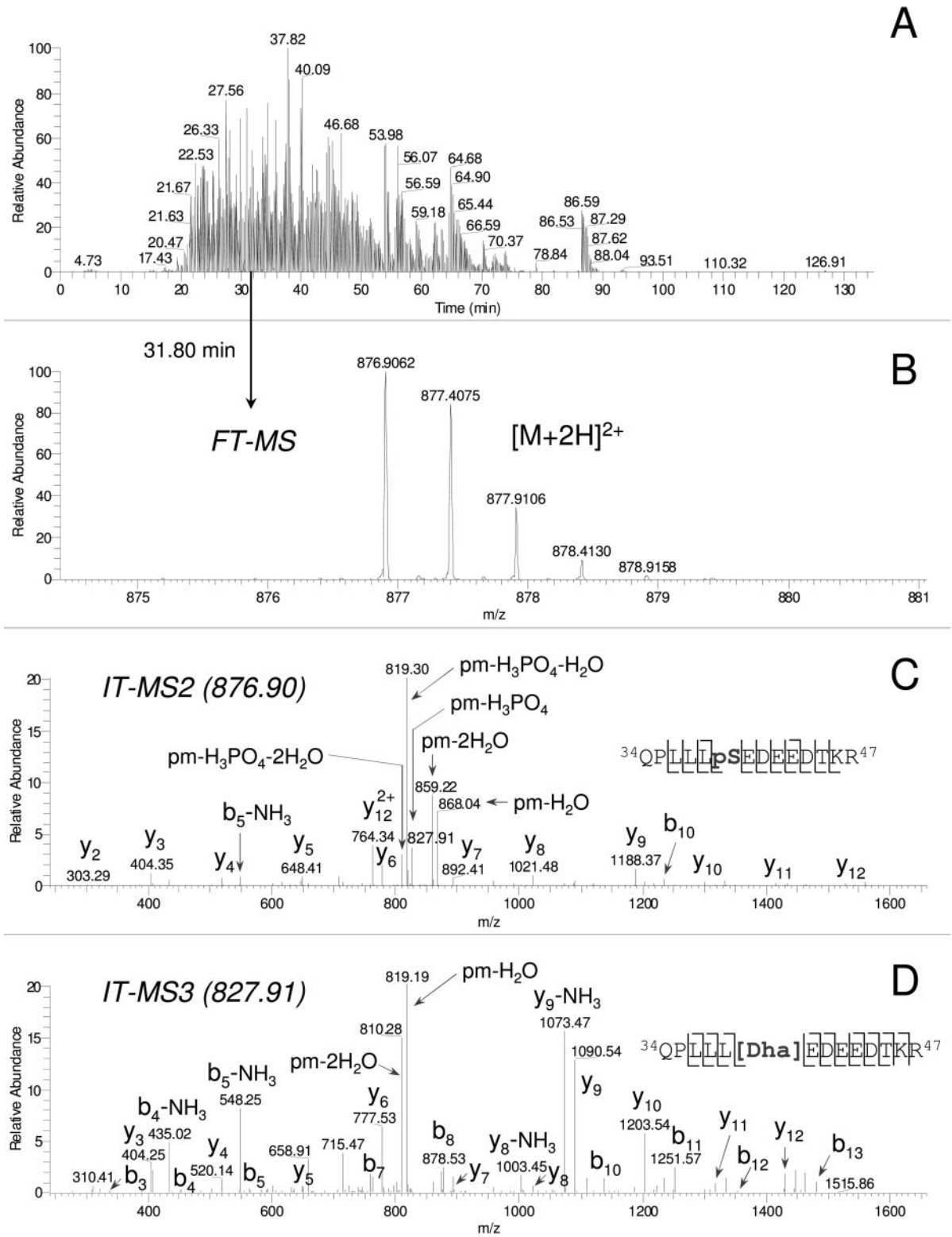

FIG. 2. **Identification of the phosphorylation site Ser-39 from eIF3c using neutral loss/MS^3 method.** *A*, base peak chromatogram. *B*, precursor mass scan at 31.8 min using FTICR (single scan from 300 to 1400 *m/z* with 100,000 resolution at 10^6 target ions). For illustration purposes, only the 875–881 *m/z* mass region of the $[M + 2H]^{2+}$ ion is shown. *C*, MS^2 scan of the *m/z* 876.90 ion. *D*, MS^3 scan of the *m/z* 827.91. The peptide sequence identified by MASCOT and validated by manual confirmation from the raw MS^2 data is shown in the *inset* of *C*. The peptide sequence validated by manual confirmation from the raw MS^3 data is shown in the *inset* of *D* where *Dha* represents the dehydroalanine residue. *Pm*, precursor ion; *IT*, ion trap; *pS*, phosphoserine.

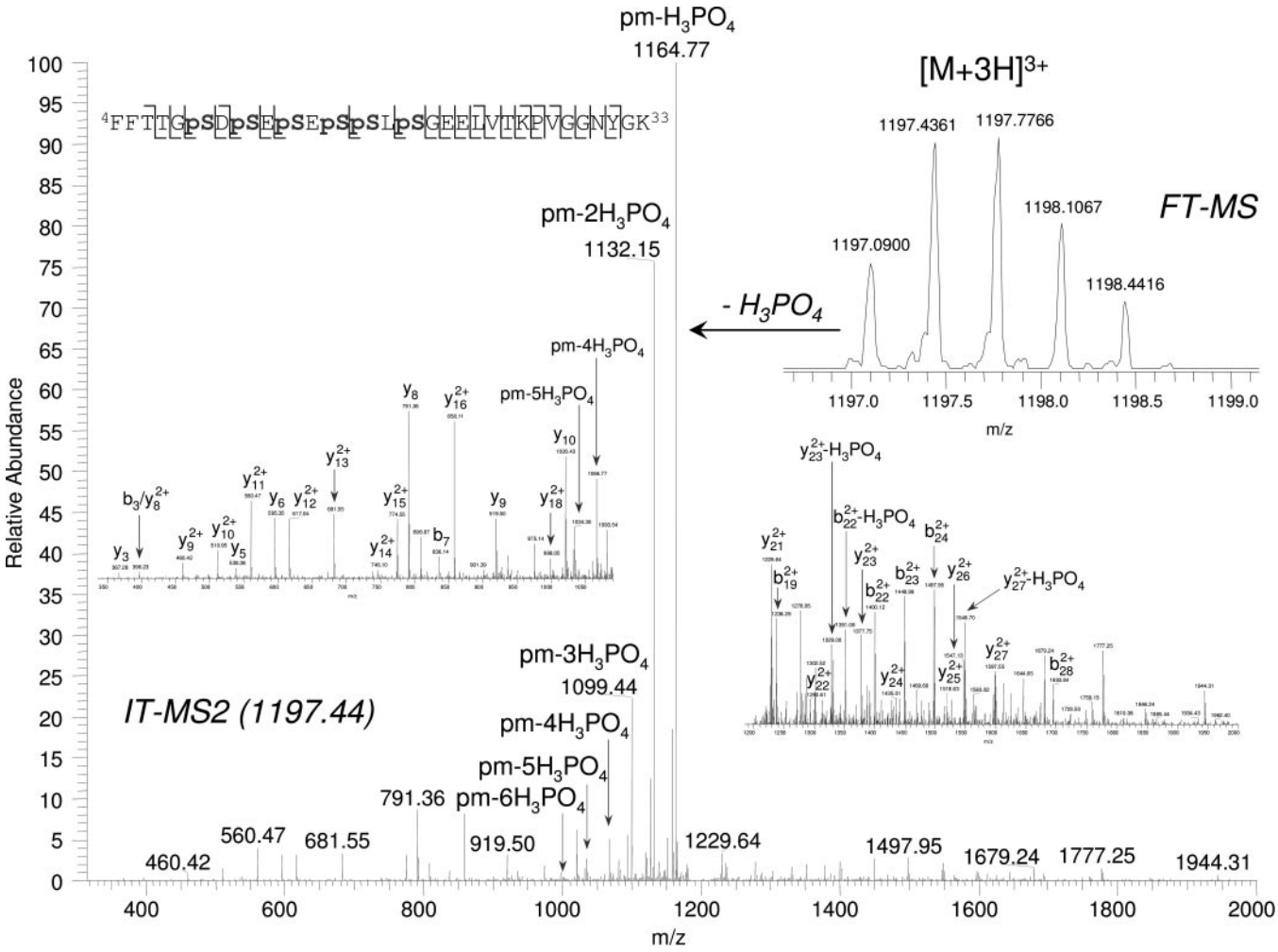

FIG. 3. **Identification of six phosphorylation sites (Ser-9, Ser-11, Ser-13, Ser-15, Ser-16, and Ser-18) from the N-terminal region of the eIF3c subunit by nano-LC-MS/MS analysis.** The FTMS survey scan revealed the $[M + 3H]^{3+}$ ion of the tryptic peptide (amino acids 4–33) with the monoisotopic mass *m/z* of 1197.0900 (*inset*, *top right*). This ion was isolated and fragmented in the linear ion trap to produce the MS^2 spectrum. The peptide sequence identified by MASCOT and validated by manual confirmation from the raw MS^2 data is shown in the *inset* (*top left*). *Pm*, precursor ion; *IT*, ion trap; *pS*, phosphoserine.

ping is a prerequisite for preparing phosphopeptide-specific antibodies and for mutating the sites, approaches that will help establish whether or not eIF3 phosphorylation plays a role in translational control. We believe that such experiments are important especially for elucidating eIF3 interactions with other translational components. We provide two specific examples of areas where eIF3 phosphorylation may be involved in regulation. eIF1 and eIF5 bind within the yeast multifactor complex to the N-terminal domain of eIF3c (19) precisely where a group of six phosphorylation sites are found. Such phosphorylation may regulate formation or stability of this complex. eIF3j is important for anchoring eIF3 to the 40 S subunit (4, 23). In quiescent lymphocytes, eIF3j is found dissociated from the eIF3 complex and ribosomes but upon lymphocyte activation becomes bound to 40 S ribosomes along with eIF3 (50). Because the association of eIF3j with eIF3 and the ribosome is blocked by rapamycin, an inhibitor of mTOR (mammalian target of rapamycin), it is likely that phosphorylation plays a role in these events. Experiments are under way to test when and to what extent specific eIF3 sites are phosphorylated and whether the modifications contribute to translational control.

Mass Spectrometric Analysis of the Intact eIF3 Protein Complex—Having identified phosphorylation sites, a second mass spectrometric approach was used to measure the mass of the intact 13-subunit complex. The use of a high mass Q-TOF type instrument (40, 41) allowed observation of the intact 13-component complex of eIF3 as shown in Fig. 4. Isolation of a narrow mass range of an undefined broad peak at *m/z* 12,200 and activation of this species revealed alongside the isolated peak the presence of clearly resolved charge states consistent with the intact eIF3 complex with each of its 13 subunits present in stoichiometric amounts. The measured molecular mass of the complex is 803,985 ± 94 Da as compared with the sum of all

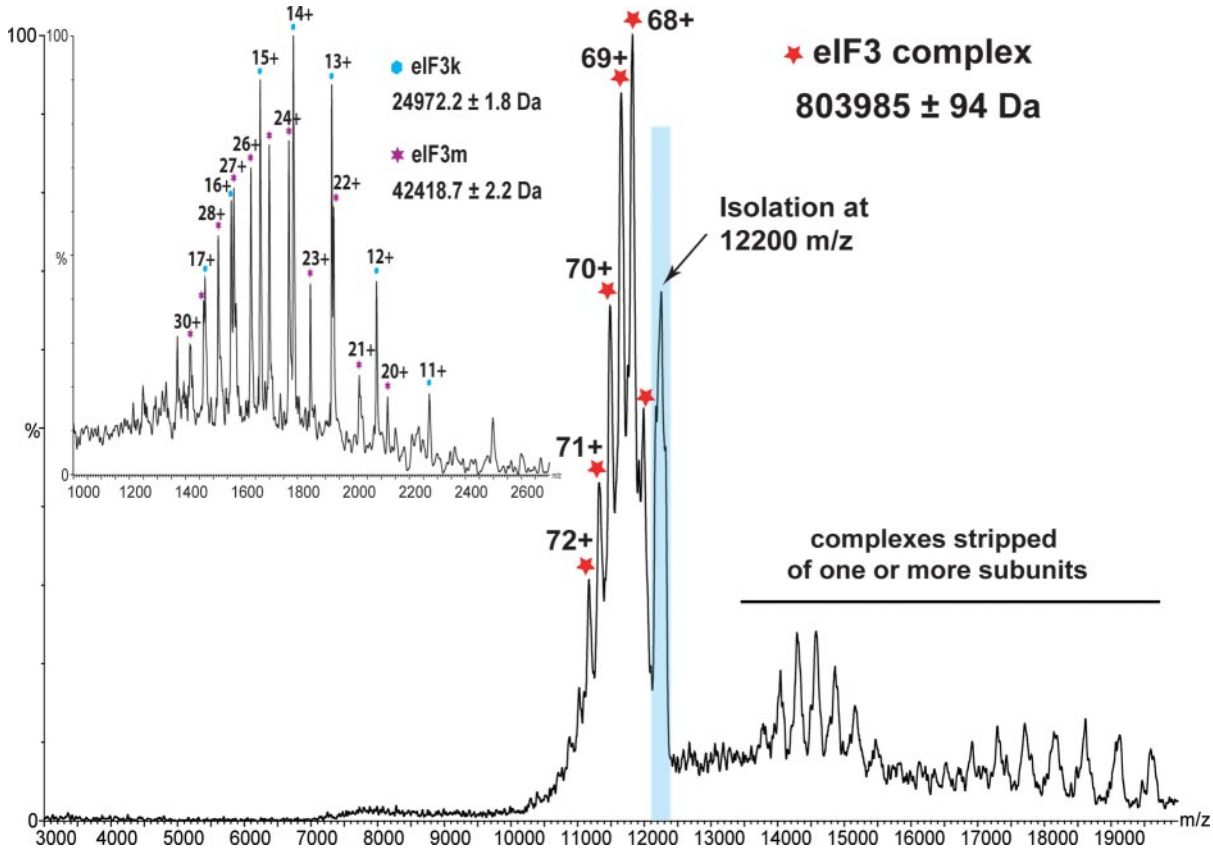

FIG. 4. **Mass spectrometric analysis of the intact eIF3 protein complex in 100 mM ammonium acetate.** Isolation and activation of *m/z* 12,200 revealed a well resolved series of charge states consistent with the intact eIF3 complex as well as the isolation peak. Loss of two subunits, eIF3k and eIF3m, from the intact complex is evident in their appearance in the low *m/z* region (see *inset*) as well as in the less highly charged complexes stripped of these subunits at high *m/z* region.

the modified proteins of 795,122.9 Da. The mass difference between measured and theoretical is 1.1% and most likely results from insufficient removal of buffers and/or solvents (51). Given the high molecular weight and complex structure, this deviation is within accepted tolerances. Detection of this complex indicates that all 13 subunits are capable of residing simultaneously in a single complex in contrast to the two distinct forms of eIF3 found in *S. pombe* (11).

Further acceleration of this isolated ion packet and tandem mass spectrometry yielded two of the component subunits, k and m (see Fig. 4, *inset*). The theoretical mass of the modified eIF3k subunit (24,970.59 Da, Table I) is in very close agreement with the experimentally measured mass (24,972.2 ± 1.8 Da). A good correlation between the experimental (42,418.7 ± 2.2 Da) and calculated mass (42,413.84 Da) of the eIF3m subunit was also obtained from the MS/MS analysis of the *m/z* 12,200 ion packet. These data in combination with higher energy collisional activation of the complex yielded the additional losses of subunits h and i (see Fig. 5 and Table I). The combined data indicate that these four subunits preferentially dissociate and therefore are likely to be on the periphery of the complex (52). It is interesting to note that the subunits that appear to occupy the outer regions of the eIF3 complex are not the proteins that are highly phosphorylated. The phosphorylated proteins do not readily dissociate and perhaps occupy the inner core portion of the complex.

The observations of the overall stoichiometry and structural organization of the human eIF3 complex have not been reported previously. However, Fraser *et al.* (4) did investigate the interactions between the human eIF3 core subunits using the baculovirus expression system. The eIF3b subunit appeared to be a central scaffolding subunit to which most, if not all, of the other eIF3 core subunits bind. Our finding of seven phosphorylation sites on eIF3b supports our proposed anchoring role of this post-translational modification. Experiments are currently underway to map all of the protein partners using high mass analysis and a variety of biochemical techniques.

Conclusions—Although first characterized in the 1970s, detailed information on the molecular structure of the mammalian initiation factor eIF3 and stoichiometry of the subunits has been lacking. Two mass spectrometric approaches were used in the present study to collect structural information about human eIF3 protein complex. In the first approach, the bottom-up analysis of the eIF3 allowed for the identification of a total of 13 protein components (eIF3a–m) with a sequence coverage of ~79%. Furthermore 29 phosphorylation sites and several other post-

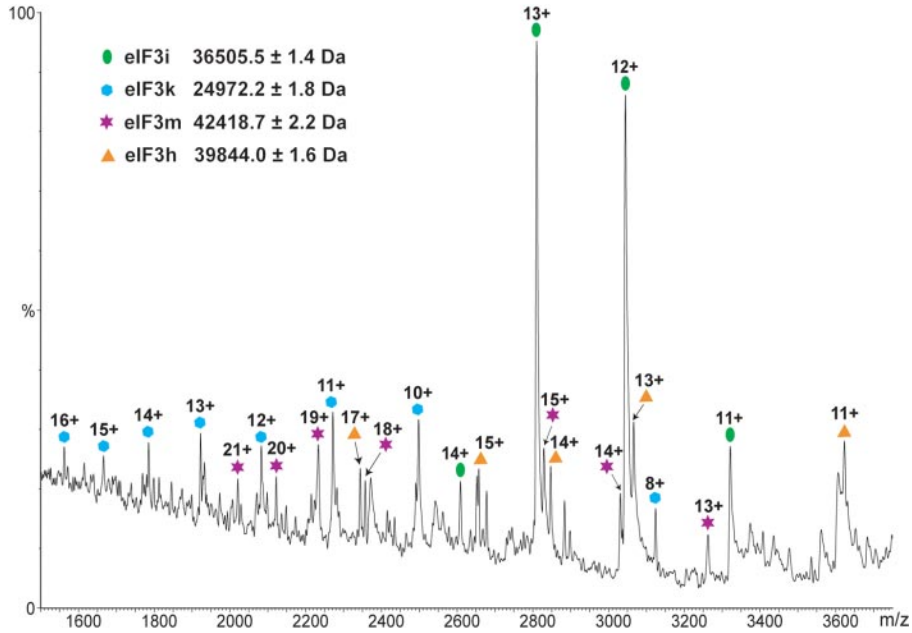

FIG. 5. **Low *m/z* region of the MS/MS spectrum recorded after collisional activation of *m/z* 12,200 assigned to the intact eIF3 complex shows the loss of four subunits (h, i, k, and m) from the intact complex.**

translational modifications were unambiguously identified within the eIF3 complex. The second mass spectrometric approach, involving analysis of intact eIF3, allowed for the first time observation of the intact 13-component complex of eIF3 with each of its 13 subunits present in stoichiometric amounts.

Four eIF3 subunits (h, i, k, and m) were found to dissociate preferentially and are therefore likely to be on the periphery of the complex. It is interesting to note that the high density of phosphorylation sites identified in this study appear to be in core subunits. The absence of these proteins among the group of peripheral subunits readily released from the intact complex implies an intriguing link between phosphorylation and location within the complex. More generally this study exemplifies the complementarity of the two mass spectrometry approaches, combining to give information on post-translational modifications as well as the subunit organization of the complex. It provides a starting point for the long term goal of discovering how phosphorylations affect the contacts and functions of eIF3 subunits within the complex and in turn govern their interactions with ribosomes.

Acknowledgments—We thank Dr. Catalina Damoc and Dr. Brett Phinney of the University of California Davis Genome Center Proteomics Core for use of the LTQ-FTICR mass spectrometer.

* This work was supported in part by National Institutes of Health Program Project Grant GM073732. The costs of publication of this article were defrayed in part by the payment of page charges. This article must therefore be hereby marked "*advertisement*" in accordance with 18 U.S.C. Section 1734 solely to indicate this fact.

S The on-line version of this article (available at http://www.mcponline.org) contains supplemental material.

** Supported by the Biotechnology and Biological Sciences Research Council.

‡‡ To whom correspondence should be addressed. Tel.: 530-754-4987; E-mail: jaleary@ucdavis.edu.

REFERENCES

1. Hershey, J. W., and Merrick, W. C. (2000) *Translational Control of Gene Expression*, pp. 33–38, Cold Spring Harbor Laboratory Press, Cold Spring Harbor, NY
2. Chaudhuri, J., Chowdhury, D., and Maitra, U. (1999) Distinct functions of eukaryotic translation initiation factors eIF1A and eIF3 in the formation of the 40 S ribosomal preinitiation complex. *J. Biol. Chem.* **274,** 17975–17980
3. Hinnebusch, A. G. (2006) eIF3: a versatile scaffold for translation initiation complexes. *Trends Biochem. Sci.* **31,** 553–562
4. Fraser, C. S., Lee, J. Y., Mayeur, G. L., Bushell, M., Doudna, J. A., and Hershey, J. W. (2004) The j-subunit of human translation initiation factor eIF3 is required for the stable binding of eIF3 and its subcomplexes to 40 S ribosomal subunits in vitro. *J. Biol. Chem.* **279,** 8946–8956
5. Lamphear, B. J., Kirchweger, R., Skern, T., and Rhoads, R. E. (1995) Mapping of functional domains in eukaryotic protein synthesis initiation factor 4G (eIF4G) with picornaviral proteases. Implications for cap-dependent and cap-independent translational initiation. *J. Biol. Chem.* **270,** 21975–21983
6. Korneeva, N. L., Lamphear, B. J., Hennigan, F. L., and Rhoads, R. E. (2000) Mutually cooperative binding of eukaryotic translation initiation factor (eIF) 3 and eIF4A to human eIF4G-1. *J. Biol. Chem.* **275,** 41369–41376
7. Pestova, T. V., Lomakin, I. B., Lee, J. H., Choi, S. K., Dever, T. E., and Hellen, C. U. (2000) The joining of ribosomal subunits in eukaryotes requires eIF5B. *Nature* **403,** 332–335
8. Browning, K. S., Gallie, D. R., Hershey, J. W., Hinnebusch, A. G., Maitra, U., Merrick, W. C., and Norbury, C. (2001) Unified nomenclature for the subunits of eukaryotic initiation factor 3. *Trends Biochem. Sci.* **26,** 284–290
9. Unbehaun, A., Borukhov, S. I., Hellen, C. U., and Pestova, T. V. (2004) Release of initiation factors from 48S complexes during ribosomal subunit joining and the link between establishment of codon-anticodon base-pairing and hydrolysis of eIF2-bound GTP. *Genes Dev.* **18,** 3078–3093
10. Mayeur, G. L., Fraser, C. S., Peiretti, F., Block, K. L., and Hershey, J. W. (2003) A newly discovered subunit of mammalian translation initiation factor eIF3. *Eur. J. Biochem.* **270,** 4133–4139
11. Zhou, C., Arslan, F., Wee, S., Krishnan, S., Ivanov, A. R., Oliva, A., Leatherwood, J., and Wolf, D. A. (2005) PCI proteins eIF3e and eIF3m define distinct translation initiation factor 3 complexes. *BMC Biol.* **3,** 14
12. Phan, L., Schoenfeld, L. W., Valasek, L., Nielsen, K. H., and Hinnebusch, A. G. (2001) A subcomplex of three eIF3 subunits binds eIF1 and eIF5 and stimulates ribosome binding of mRNA and tRNA(i)Met. *EMBO J.* **20,**

2954–2965
13. Asano, K., Phan, L., Anderson, J., and Hinnebusch, A. G. (1998) Complex formation by all five homologues of mammalian translation initiation factor 3 subunits from yeast Saccharomyces cerevisiae. *J. Biol. Chem.* **273,** 18573–18585
14. Das, S., Maiti, T., Das, K., and Maitra, U. (1997) Specific interaction of eukaryotic translation initiation factor 5 (eIF5) with the β-subunit of eIF2. *J. Biol. Chem.* **272,** 31712–31718
15. Bandyopadhyay, A., and Maitra, U. (1999) Cloning and characterization of the p42 subunit of mammalian translation initiation factor 3 (eIF3): demonstration that eIF3 interacts with eIF5 in mammalian cells. *Nucleic Acids Res.* **27,** 1331–1337
16. Majumdar, R., Bandyopadhyay, A., and Maitra, U. (2003) Mammalian translation initiation factor eIF1 functions with eIF1A and eIF3 in the formation of a stable 40 S preinitiation complex. *J. Biol. Chem.* **278,** 6580–6587
17. Methot, N., Song, M. S., and Sonenberg, N. (1996) A region rich in aspartic acid, arginine, tyrosine, and glycine (DRYG) mediates eukaryotic initiation factor 4B (eIF4B) self-association and interaction with eIF3. *Mol. Cell. Biol.* **16,** 5328–5334
18. Imataka, H., and Sonenberg, N. (1997) Human eukaryotic translation initiation factor 4G (eIF4G) possesses two separate and independent binding sites for eIF4A. *Mol. Cell. Biol.* **17,** 6940–6947
19. Asano, K., Clayton, J., Shalev, A., and Hinnebusch, A. G. (2000) A multifactor complex of eukaryotic initiation factors, eIF1, eIF2, eIF3, eIF5, and initiator tRNA(Met) is an important translation initiation intermediate in vivo. *Genes Dev.* **14,** 2534–2546
20. Valasek, L., Nielsen, K. H., and Hinnebusch, A. G. (2002) Direct eIF2-eIF3 contact in the multifactor complex is important for translation initiation in vivo. *EMBO J.* **21,** 5886–5898
21. Fletcher, C. M., Pestova, T. V., Hellen, C. U., and Wagner, G. (1999) Structure and interactions of the translation initiation factor eIF1. *EMBO J.* **18,** 2631–2637
22. Bieniossek, C., Schutz, P., Bumann, M., Limacher, A., Uson, I., and Baumann, U. (2006) The crystal structure of the carboxy-terminal domain of human translation initiation factor eIF5. *J. Mol. Biol.* **360,** 457–465
23. Nielsen, K. H., Valasek, L., Sykes, C., Jivotovskaya, A., and Hinnebusch, A. G. (2006) Interaction of the RNP1 motif in PRT1 with HCR1 promotes 40S binding of eukaryotic initiation factor 3 in yeast. *Mol. Cell. Biol.* **26,** 2984–2998
24. Park, H. S., Browning, K. S., Hohn, T., and Ryabova, L. A. (2004) Eucaryotic initiation factor 4B controls eIF3-mediated ribosomal entry of viral reinitiation factor. *EMBO J.* **23,** 1381–1391
25. Lefebvre, A. K., Korneeva, N. L., Trutschl, M., Cvek, U., Duzan, R. D., Bradley, C. A., Hershey, J. W., and Rhoads, R. E. (2006) Translation initiation factor eIF4G-1 binds to eIF3 through the eIF3e subunit. *J. Biol. Chem.* **281,** 22917–22932
26. Siridechadilok, B., Fraser, C. S., Hall, R. J., Doudna, J. A., and Nogales, E. (2005) Structural roles for human translation factor eIF3 in initiation of protein synthesis. *Science* **310,** 1513–1515
27. Srivastava, S., Verschoor, A., and Frank, J. (1992) Eukaryotic initiation factor 3 does not prevent association through physical blockage of the ribosomal subunit-subunit interface. *J. Mol. Biol.* **226,** 301–304
28. Hershey, J. W. (1989) Protein phosphorylation controls translation rates. *J. Biol. Chem.* **264,** 20823–20826
29. Dever, T. E. (2002) Gene-specific regulation by general translation factors. *Cell* **108,** 545–556
30. Hunt, D. L., Yates, J. R., III, Shabanowitz, J., Winston, S., and Hauer, C. R. (1986) Protein sequencing by tandem mass spectrometry. *Proc. Natl. Acad. Sci. U. S. A.* **83,** 6233–6237
31. Link, A., Eng, J., Schieltz, D. M., Carmack, E., Mize, G. J., Morris, D. R., Garvik, B. M., and Yates, J. R., III (1999) Direct analysis of protein complexes using mass spectrometry. *Nat. Biotechnol.* **17,** 676–682
32. Miranker, A., Robinson, C. V., Radford, S. E., Aplin, R. T., and Dobson, C. M. (1993) Detection of transient protein folding populations by mass spectrometry. *Science* **262,** 896–900
33. Heck, A. J. R., and van den Heuvel, R. H. H. (2004) Investigation of intact protein complexes by mass spectrometry. *Mass Spectrom. Rev.* **23,** 368–389
34. Yu, Y., Sweeney, M. D., Saad, O. M., Crown, S. E., Hsu, A. R., Handel, T. M., and Leary, J. A. (2005) Chemokine-glycosaminoglycan binding. Specificity for CCR2 ligand binding to highly sulfated oligosaccharides using FTICR mass spectrometry. *J. Biol. Chem.* **280,** 32200–32208
35. Davis, M. T., and Lee, T. D. (1998) Rapid protein identification using a microscale electrospray LC/MS system on an ion trap mass spectrometer. *J. Am. Soc. Mass Spectrom.* **9,** 194–201
36. Figeys, D., Ducret, A., and Aebersold, R. (1997) Identification of proteins by capillary electrophoresis-tandem mass spectrometry evaluation of an on-line solid-phase extraction device. *J. Chromatogr. A* **763,** 295–306
37. Benesch, J. L., and Robinson, C. V. (2006) Mass spectrometry of macromolecular assemblies: preservation and dissociation. *Curr. Opin. Struct. Biol.* **16,** 245–251
38. Hernandez, H., Dziembowski, A., Taverner, T., Seraphin, B., and Robinson, C. V. (2006) Subunit architecture of multimeric complexes isolated directly from cells. *EMBO Rep.* **7,** 605–610
39. Pinkse, M. W., Uitto, P. M., Hilhorst, M. J., Ooms, B., and Heck, A. J. (2004) Selective isolation at the femtomole level of phosphopeptides from proteolytic digests using 2D-NanoLC-ESI-MS/MS and titanium oxide precolumns. *Anal. Chem.* **76,** 3935–3943
40. Sobott, F., Hernandez, H., McCammon, M. G., Tito, M. A., and Robinson, C. V. (2002) A tandem mass spectrometer for improved transmission and analysis of large macromolecular assemblies. *Anal. Chem.* **74,** 1402–1407
41. Chernushevich, I. V., and Thomson, B. A. (2004) Collisional cooling of large ions in electrospray mass spectrometry. *Anal. Chem.* **76,** 1754–1760
42. Synowsky, S. A., van den Heuvel, R. H. H., Mohammed, S., Pijnappel, W. W. M. P., and Heck, A. J. R. (2006) Probing genuine strong interactions and post-translational modifications in the heterogeneous yeast exosome protein complex. *Mol. Cell. Proteomics* **5,** 1581–1592
43. Morley, S. J., and Traugh, J. A. (1990) Differential stimulation of phosphorylation of initiation factors eIF-4F, eIF-4B, eIF-3, and ribosomal protein S6 by insulin and phorbol esters. *J. Biol. Chem.* **265,** 10611–10616
44. Scheel, H., and Hofmann, K. (2005) Prediction of a common structural scaffold for proteasome lid, COP9-signalosome and eIF3 complexes. *BMC Bioinformatics* **6,** 71
45. Beausoleil, S. A., Jedrychowski, M., Schwartz, D., Elias, J. E., Villen, J., Li, J., Cohn, M. A., Cantley, L. C., and Gygi, S. P. (2004) Large-scale characterization of HeLa cell nuclear phosphoproteins. *Proc. Natl. Acad. Sci. U. S. A.* **101,** 12130–12135
46. Gevaert, K., Staes, A., Van Damme, J., De Groot, S., Hugelier, K., Demol, H., Martens, L., Goethals, M., and Vandekerckhove, J. (2005) Global phosphoproteome analysis on human HepG2 hepatocytes using reversed-phase diagonal LC. *Proteomics* **5,** 3589–3599
47. Kim, J., Tannenbaum, S., and White, F. (2005) Global phosphoproteome of HT-29 human colon adenocarcinoma cells. *J. Proteome Res.* **4,** 1339–1346
48. Gruhler, A., Olsen, J. V., Mohammed, S., Mortensen, P., Faergeman, N. J., Mann, M., and Jensen, O. N. (2005) Quantitative phosphoproteomics applied to the yeast pheromone signaling pathway. *Mol. Cell. Proteomics* **4,** 310–327
49. Shi, J., Feng, Y., Goulet, A. C., Vaillancourt, R. R., Sachs, N. A., Hershey, J. W., and Nelson, M. A. (2003) The p34cdc2-related cyclin-dependent kinase 11 interacts with the p47 subunit of eukaryotic initiation factor 3 during apoptosis. *J. Biol. Chem.* **278,** 5062–5071
50. Miyamoto, S., Patel, P., and Hershey, J. W. (2005) Changes in ribosomal binding activity of eIF3 correlate with increased translation rates during activation of T lymphocytes. *J. Biol. Chem.* **280,** 28251–28264
51. McKay, A. R., Ruotolo, B. T., Ilag, L. L., and Robinson, C. V. (2006) Mass measurements of increased accuracy resolve heterogeneous populations of intact ribosomes. *J. Am. Chem. Soc.* **128,** 11433–11442
52. Sharon, M., Taverner, T., Ambroggio, X. I., Deshaies, R. J., and Robinson, C. V. (2006) Structural organization of the 19S proteasome lid: insights from MS of intact complexes. *PLoS Biol.* **4,** 1314–1323
53. Obenauer, J. C., Cantley, L. C., and Yaffe, M. B. (2003) Scansite 2.0: proteome-wide prediction of cell signaling interactions using short sequence motifs. *Nucleic Acids Res.* **31,** 3635–3641